Ferrata Storti Foundation

Haematologica 2019
Volume 104(7):1332-1341

NIPBL: a new player in myeloid cell differentiation

Mara Mazzola,[1]* Gianluca Deflorian,[2]* Alex Pezzotta,[1] Laura Ferrari,[2] Grazia Fazio,[3] Erica Bresciani,[4] Claudia Saitta,[3] Luca Ferrari,[1] Monica Fumagalli,[5] Matteo Parma,[5] Federica Marasca,[6] Beatrice Bodega,[6] Paola Riva,[1] Franco Cotelli,[7] Andrea Biondi,[3] Anna Marozzi,[1] Gianni Cazzaniga[3] and Anna Pistocchi[1]

[1]Dipartimento di Biotecnologie Mediche e Medicina Traslazionale, Università degli Studi di Milano, LITA, Segrate, Italy; [2]Istituto FIRC di Oncologia Molecolare, IFOM, Milano, Italy; [3]Centro Ricerca Tettamanti, Clinica Pediatrica Università di Milano-Bicocca, Centro Maria Letizia Verga, Monza, Italy; [4]Oncogenesis and Development Section, National Human Genome Research Institute, National Institutes of Health, Bethesda, MD, USA; [5]Clinica Ematologica e Centro Trapianti di Midollo Osseo, Ospedale San Gerardo, Università di Milano-Bicocca, Monza, Italy; [6]Istituto Nazionale di Genetica Molecolare "Romeo ed Enrica Invernizzi" (INGM), Milano, Italy and [7]Dipartimento di Bioscienze, Università degli Studi di Milano, Milano, Italy.

** MM and GDF contributed equally to this work*

ABSTRACT

The nucleophosmin 1 gene (*NPM1*) is the most frequently mutated gene in acute myeloid leukemia. Notably, *NPM1* mutations are always accompanied by additional mutations such as those in cohesin genes *RAD21*, *SMC1A*, *SMC3*, and *STAG2* but not in the cohesin regulator, nipped B-like (*NIPBL*). In this work, we analyzed a cohort of adult patients with acute myeloid leukemia and *NPM1* mutation and observed a specific reduction in the expression of *NIPBL* but not in other cohesin genes. In our zebrafish model, overexpression of the mutated form of *NPM1* also induced downregulation of *nipblb*, the zebrafish ortholog of human *NIPBL*. To investigate the hematopoietic phenotype and the interaction between mutated *NPM1* and *nipblb*, we generated a zebrafish model with *nipblb* downregulation which showed an increased number of myeloid progenitors. This phenotype was due to hyper-activation of the canonical Wnt pathway: myeloid cells blocked in an undifferentiated state could be rescued when the Wnt pathway was inhibited by *dkk1b* mRNA injection or indomethacin administration. Our results reveal, for the first time, a role for *NIPBL* during zebrafish hematopoiesis and suggest that an interplay between *NIPBL/NPM1* may regulate myeloid differentiation in zebrafish and humans through the canonical Wnt pathway and that dysregulation of these interactions may drive leukemic transformation.

Correspondence:

ANNA PISTOCCHI
anna.pistocchi@unimi.it

Received: July 5, 2018.

Accepted: January 3, 2019.

Pre-published: January 10, 2019.

doi:10.3324/haematol.2018.200899

Check the online version for the most updated information on this article, online supplements, and information on authorship & disclosures: www.haematologica.org/content/104/7/1332

©2019 Ferrata Storti Foundation

Material published in Haematologica is covered by copyright. All rights are reserved to the Ferrata Storti Foundation. Use of published material is allowed under the following terms and conditions: https://creativecommons.org/licenses/by-nc/4.0/legalcode. Copies of published material are allowed for personal or internal use. Sharing published material for non-commercial purposes is subject to the following conditions: https://creativecommons.org/licenses/by-nc/4.0/legalcode, sect. 3. Reproducing and sharing published material for commercial purposes is not allowed without permission in writing from the publisher.

Introduction

Acute myeloid leukemia (AML) is an aggressive hematologic malignancy of bone marrow characterized by the accumulation of immature myeloid blasts that show defective differentiation and function.[1,2] Advances in cancer genomics have shown that relatively few recurrent somatic mutations give rise to human AML, with an average of five mutations in each case of *de novo* AML.[3] These somatic mutations, which collectively determine the malignant phenotype, are serially acquired in clones of self-renewing hematopoietic stem cells (HSC), termed pre-leukemic HSC.[4] The genes mutated in HSC that are relevant in the pathogenesis of AML have been divided into nine categories, including transcription-factor fusions, nucleophosmin (*NPM1*), tumor-suppressor genes, DNA-methylation–related genes, signaling genes, chromatin-modifying genes, myeloid transcription-factor genes, cohesin-complex genes and spliceosome-complex genes.[5]

NPM1, the most frequently mutated gene in AML, is a phosphoprotein that normally resides in the nucleolus.[6,7] More than 50 different reported mutations in human *NPM1* result in aberrant cytoplasmic translocation of the protein, named

NPMc+, which functions as an oncogene *in vitro*[8] and has a role in aberrant hematopoiesis *in vivo*. Indeed, murine models expressing *NPMc+* in the hematopoietic lineage develop myeloproliferative disease[9] and leukemia[10,11] while the forced expression of human *NPMc+* in zebrafish causes an increase in primitive early myeloid cells and definitive hematopoietic stem cells (HSC).[12,13] It has also been demonstrated, with similar results in zebrafish and human AML blasts, that the expression of *NPMc+* activates canonical Wnt signaling, providing insight into the molecular pathogenesis of AML bearing *NPM1* mutations.[12] Indeed, the canonical Wnt/β-catenin pathway has been shown to be crucial for the regulation of HSC proliferation, differentiation and apoptosis.[14]

Recently, mutations in cohesin genes were found to be strongly correlated with *NPM1* mutations although they do not seem to affect the prognosis of patients with AML.[15] The cohesin complex is composed of different proteins that form a complex (SMC1, SMC3, RAD21, STAG1 and STAG2), and by additional regulator proteins (NIPBL, MAU2, ESCO1, ESCO2 and HDAC8). This multifunctional complex regulates the cohesion of sister chromatids during cell division, but also gene transcription and chromatin architecture. Recently, the genes of the cohesin complex were found to be mutated in almost 10% of patients with myeloid malignancies, while an additional 15% of patients had reduced expression of cohesin transcripts, suggesting a role for the cohesin complex in the pathogenesis of AML.[5] In a cohort of patients studied by Thota and colleagues,[15] the most frequently mutated genes of the cohesin complex were *STAG2* (5.9%), *RAD21* (2%), and *SMC3* (2%), whereas mutations in the other cohesins were less frequent (<1%). Somatic mutations in cohesin subunits are mutually exclusive and, being mainly nonsense and frameshift mutations, result in a predicted loss-of-function phenotype.[16] It should be noted that cohesin mutations in AML, but not in other kind of tumors,[17] are associated with a normal karyotype in malignant cells; therefore, the role of cohesins in tumor development is not correlated with their function in sister chromatid cohesion but rather with their role in mediating DNA accessibility to gene regulatory elements.[15] Indeed, *in vitro* and *in vivo* models of cohesin haploinsufficiency show a delay in the differentiation of HSC, which are expanded in an immature state.[18-21]

In this work, we studied the expression of cohesin genes in a cohort of adults with AML and found a specific downregulation of *NIPBL* when *NPM1* was mutated. Interestingly, we also found that *nipblb* was downregulated in our zebrafish model for *NPMc+* expression. The zebrafish (*Danio rerio*) is a powerful model for studying hematologic diseases as it shares several hematopoietic genes with higher vertebrates, and mutations in human leukemia-causative genes disrupt normal hematopoiesis in zebrafish, suggesting a functional conservation of these genes during evolution. Our zebrafish model with loss-of-function of *nipblb* showed dysregulation of myeloid cell differentiation with increased numbers of myeloid precursors and a decrease of mature myeloid cells. The hematopoietic phenotype presented by *nipblb*-loss-of-function zebrafish embryos recapitulated the myeloid defects presented by embryos with *NPMc+* overexpression and was due to hyper-activation of the canonical Wnt pathway. Indeed, overexpression of the *dkk1b* Wnt inhibitor or indomethacin treatment rescued the phenotype.

Our study provides new insights into the molecular mechanisms underlying *NIPBL* function, identifying the canonical Wnt pathway as one of its targets and indicating that it plays a role with *NPMc+* in the development of AML. Using the well-suited zebrafish model, we established a platform to further investigate the mechanisms through which *NPMc+* and *NIPBL* might interact and contribute to leukemic transformation.

Methods

Patients

Diagnostic bone marrow samples from healty subjects and 40 adult patients affected by AML were collected and characterized as described in the *Online Supplementary Methods*. Patients' material was collected after obtaining informed consent (protocol ASG-MA-052A approved on May 8th, 2012 by Azienda San Gerardo). The clinical features of the participants are reported in *Online Supplementary Table S1*. Human material and derived data were used in accordance with the Declaration of Helsinki.

Animals

Zebrafish embryos were raised and maintained according to international (European Union Directive 2010/63/EU) and national (Italian decree n. 26 of March 4th, 2014) guidelines on the protection of animals used for scientific purposes, as described in the *Online Supplementary Methods*.

Reverse transcription and real-time quantitative polymerase chain reaction assays

RNA was extracted from human and zebrafish embryos using TRIZOL reagents (Life Technologies, Carlsbad, CA, USA), following the manufacturer's protocol. Quantitative reverse transcriptase polymerase chain reaction (RT-PCR) experiments on human samples were performed with the Universal Probe Library system (Roche Diagnostics, Basel, Swiss), as described in the *Online Supplementary Methods*. Probes and primers are reported in *Online Supplementary Tables S2 and S3*.

Western blotting

Protein extracts were prepared, loaded and quantified as described in the *Online Supplementary Methods*. The antibodies used are listed in *Online Supplementary Table S4*. Images were acquired using an Alliance MINI HD9 AUTO Western Blot Imaging System (UVItec Limited, Cambridge, UK) and analyzed with the related software.

In situ hybridization and immunofluorescent analyses

Whole mount *in situ* hybridization (WISH) experiments, were carried out as described by Thisse *et al.*[22] and in the *Online Supplementary Methods*. Pictures were acquired with a Leica DFC480 photo camera (Leica, Wetzlar, Germany). Immunostaining was performed as described previously.[23] The antibodies used are listed in *Online Supplementary Table S4*. Images were acquired as described in the *Online Supplementary Methods*.

Sudan black staining

Sudan black staining was performed as described by Cvejic *et al.*[24] and in the *Online Supplementary Methods*.

Fluorescence-activated cell sorting analyses

Embryo dissociation was performed as described previously.[25] Fluorescence-activated cell sorting (FACS) analyses were performed as described in the *Online Supplementary Methods* on

Tg(CD41:GFP) zebrafish embryos at 3 days post-fertilization (dpf) or PU.1-stained cells derived from embryos at 3 dpf.

Injections and indomethacin treatment

Injections were carried out on one- to two-cell stage embryos. Morpholinos were injected as described in the *Online Supplementary Methods*. Human *NPM1* and *NPMc+* and zebrafish *dkk1b* mRNA were generated as previously described[12] and injected as detailed in the *Online Supplementary Methods.* Indomethacin (Sigma-Aldrich St. Louis, MO, USA) treatment was administered as described by North *et al.*[26]

Confocal imaging

Previously immunostained 3 dpf embryos were equilibrated and mounted in 85% glycerol solution in phosphate-buffered saline and imaged using a TCS-SP2 confocal microscope (Leica), with 40X oil immersion objective, 488 nm argon ion and 405 nm diode lasers. For each sample, single stack images were acquired.

Statistical analyses

For quantitative RT-PCR experiments, data were statistically analyzed applying one-way analysis of variance (ANOVA) or *t*-tests, defining $P \leq 0.05$ (*), $P \leq 0.01$ (**), and $P \leq 0.001$ (***) as statistically significant values.[27] Data were analyzed using the comparative ΔΔCt method. Both t- test and standard deviation (SD) values refer to data from triplicate samples. In zebrafish at least three different experiments were done for each analysis. For cell counts and phenotypic analyses, statistical analysis was performed by the χ^2 test, with Yates correction when needed.

Results

Cohesin expression in subgroups of adult patients with acute myeloid leukemia carrying *NPM1* mutations and in a zebrafish model of *NPMc+* expression

It was recently reported that somatic mutations in cohesin genes are frequently associated with *NPM1* mutations,[28] but not with other common AML mutations; however, the expression levels of cohesins have never been analyzed. We, therefore, decided to investigate the presence of alterations in the expression of cohesin genes in a cohort of 40 adult AML patients stratified into two homogeneous molecular subgroups according to the absence or presence of a *NPM1* mutation (*NPMc+*). Each subgroup was analyzed by means of quantitative RT-PCR for the expression of the cohesin genes *SMC1A*, *SMC3*, *NIPBL* and *RAD21* (Figure 1A-D). Interestingly, only *NIPBL* showed a significantly decreased expression in AML patients carrying a *NPM1* mutation (Figure 1B). Conversely, when the same patients were divided into subgroups depending on the presence or absence of a *FLT3*-internal tandem duplication (ITD), none of the cohesin genes analyzed was differently expressed between the two subgroups (*Online Supplementary Figure S1*).

We also used quantitative RT-PCR to analyze the expression of cohesin genes in a previously generated and well-characterized zebrafish model with human *NPMc+* overexpression.[12,13] The injection of 100 pg/embryo of *NPMc+* transcript led to a significant downregulation of *nipblb* in the whole embryo at 3 dpf, while the expression of other cohesin genes analyzed was unaltered or even increased (Figure 1E). We performed a stage-dependent analysis to determine at which developmental stage the overexpression of *NPMc+* started to downregulate *nipblb* expression in the whole embryo. We observed a significant decrease of *nipblb* expression starting from 48 hours post-fertilization (hpf), while no differential decreases between controls and *NPMc+* mRNA-injected embryos were observed at 24 and 36 hpf (Figure 1F). To further verify that the downregulation of zebrafish *nipblb* was strictly dependent on the forced expression of *NPMc+*, we injected different doses of the *NPMc+* transcript (25 pg/embryo, 75 pg/embryo and 125 pg/embryo) and found a significant inverse correlation between reduced *nipblb* expression and increased *NPMc+* (Figure 1G). Moreover, western blot studies of embryos at 3 dpf confirmed that the injection of *NPMc+* mRNA, at a dose of 100 pg/embryo, caused a reduction of the level of Nipbl protein in comparison to the level in control-injected embryos (Figure 1H).

nipblb loss-of-function and NPMc+ overexpression generate hematopoietic defects in zebrafish embryos

Since *NIPBL* is downregulated in AML patients in association with *NPM1* mutations, we wondered whether *nipblb* knockdown might generate defects in myeloid cell differentiation. To investigate this hypothesis, we downregulated *nipblb* in zebrafish by injecting a *nipblb* antisense morpholino targeting the ATG region (*nipblb*-MO), as previously described for the knockdown of the Nipbl protein.[29,30] In AML patients, HSC and immature myeloid blasts are increased. Therefore, to screen for myeloid defects in conditions resembling those of AML patients, we analyzed the same cell populations in *nipblb*-MO injected embryos. Knockdown of *nipblb* did not lead to significant differences in the HSC, as shown by confocal images of the caudal hematopoietic tissues (CHT) of *Tg(CD41:GFP)* embryos[31] at 3 dpf (Figure 2A,B) and by cytofluorimetric analyses to quantify the CD41:GFP^{low} HSC cells in comparison to those in controls (Figure 2D,E,G). On the other hand, at the same stage, *nipblb*-MO injected embryos showed an increase of myeloid progenitors, positive for the PU.1 antibody (Figure 2H,I; FACS in K,L,N). These observations were also confirmed by means of WISH techniques with the HSC marker *cmyb* and the myeloid progenitor marker *spi1b* with relative quantifications of the observed phenotypes, and RT-qPCR analyses (*Online Supplementary Figure S2*). Moreover, to verify whether the increased myeloid cells were blocked in an undifferentiated state, we used Sudan black staining to visualize mature myeloid cells.[24] At 4 dpf we observed a reduction of neutrophils (Figure 2O,P).

It was previously reported that the forced expression of human *NPMc+* in zebrafish embryos increased the HSC population at 30-36 hpf.[13] To further analyze whether the hematopoietic defects are still present later during hematopoiesis and are extended to myeloid cells, we injected the embryos with *NPMc+* mRNA (100 pg/embryo) and analyzed the hematopoietic phenotype. The CD41:GFP^{low} cells in the CHT of *NPMc+*-injected embryos were expanded in comparison to those in the controls (Figure 2A,C; FACS in D,F,G), as were PU.1-positive myeloid precursors (Figure 2H,J; FACS in K,M,N). Sudan black staining showed a decrease in mature myeloid cells in *NPMc+*-injected embryos in comparison to those in controls (Figure 2O,Q). Moreover, the expression levels of *cmyb* and *spi1b,* investigated by WISH and quantitative RT-PCR techniques, corroborated our previous findings (*Online Supplementary Figure S3*).

To confirm the specificity of the hematopoietic defects

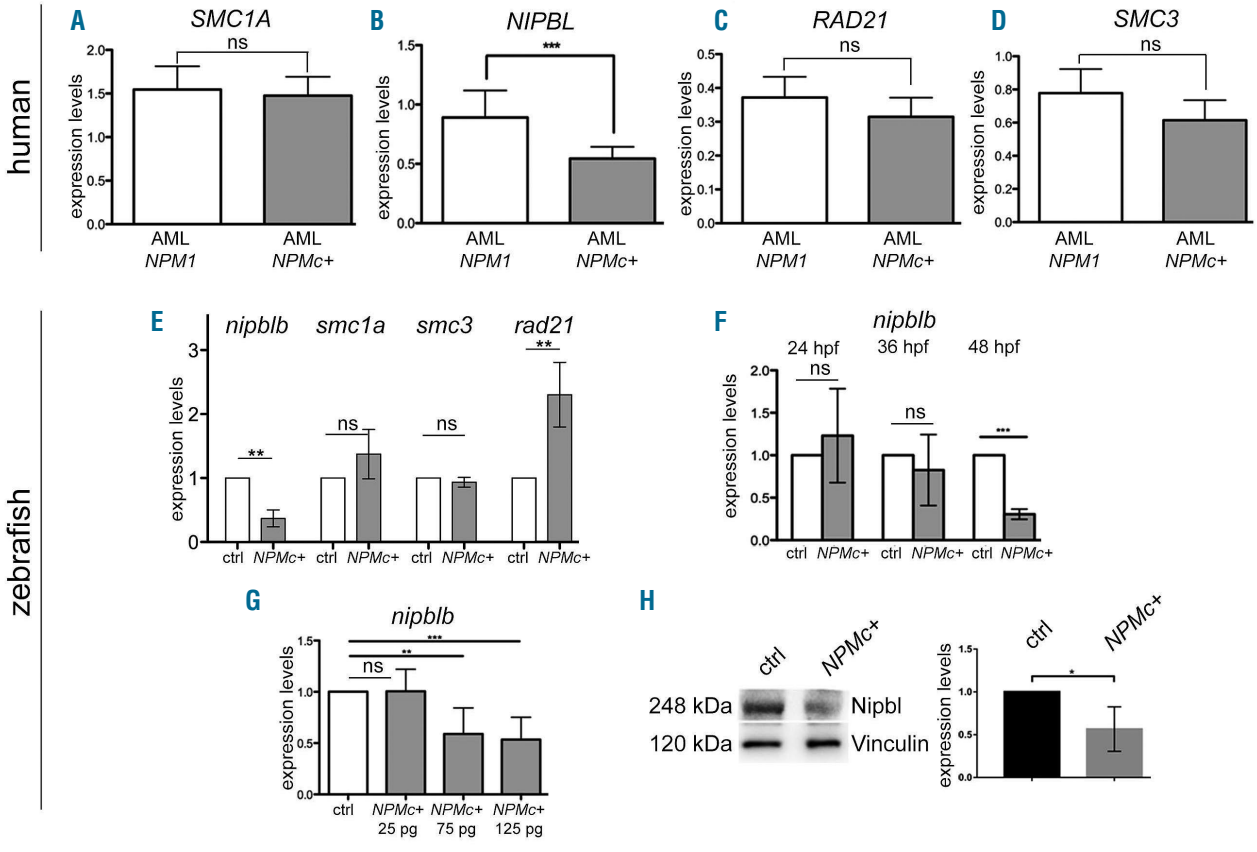

Figure 1. Expression of cohesin genes in bone marrow samples from adults with acute myeloid leukemia divided into two subgroups according to the absence or presence of *NPM1* mutations and in a zebrafish model for *NPM1* mutation (NPMc+). (A-D) Quantitative reverse transcriptase polymerase chain reaction (RT-qPCR) analyses in 40 adults with acute myeloid leukemia indicated that the expression of *NIPBL* was decreased when *NPM1* was mutated. The expression levels of the other cohesin genes analyzed did not correlate with the presence of *NPM1* mutations. (E) RT-qPCR analyses of cohesin gene expression in a zebrafish model with overexpression of human *NPMc*+ showed that the expression of *nipblb* was downregulated in comparison to that of controls at 3 days post-fertilization (dpf). (F) RT-qPCR time course analyses at 24, 36 and 48 hours post-fertilization (hpf) of *nipblb* expression in embryos injected with *NPMc*+ transcript. *nipblb* was significantly downregulated at 48 hpf. (G) RT-qPCR analyses of *nipblb* expression in zebrafish embryos at 3 dpf injected with different doses of human *NPMc*+. The downregulation of *nipblb* was significantly dependent on the dose of *NPMc*+ injected. (H) Western blot analyses of Nipbl protein expression in embryos at 3 dpf injected with 100 pg/embryo of *NPMc*+ transcript. Vinculin marker was used for normalization. Western blot images were processed as described in the *Online Supplementary Methods*. **P*<0.05, ***P*<0.01 and ****P*<0.001. ns: non-significant; AML: acute myeloid leukemia; MO: morpholino; ctrl: control.

obtained with *nipblb*-MO injection, we used a second morpholino targeting the 5'UTR region of *nipblb* (5'UTR*nipblb*-MO), which has been previously used and validated.[29] The injection of this second morpholino reduced the Nipbl protein levels, as determined by western blot analyses, confirming its efficacy in blocking protein production. It also recapitulated the hematopoietic defects observed with the injection of the ATG morpholino, showing an increased number of myeloid precursors positive for *spi1b* and a decreased number of mature myeloid cells. Moreover, when co-injected at subcritical doses, the two *nipblb*-MO cooperated to induce the myeloid phenotype (*Online Supplementary Figure S4*).

nipbl downregulation and *NPMc*+ overexpression both induce the hyper activation of the canonical Wnt pathway

Previous experimental and clinical evidence suggested a close correlation between AML development and canonical Wnt pathway dysregulation, especially in patients with *NPM1* mutations.[12] To examine whether *nipblb* and *NPMc*+ regulate the activation status of the canonical Wnt pathway, we used the *Tg(TOPdGFP)* transgenic line that bears the GFP reporter gene under the control of four enhancers and the basal promoter of *lef1*, a β-catenin-dependent transcription factor.[32] *Tg(TOPdGFP)* embryos were injected with *nipblb*-MO or *NPMc*+ mRNA and the expression of *gfp* and *axin2*, one of the direct targets of activated β-catenin, were analyzed by quantitative RT-PCR at 3 dpf.[33] Both genes were upregulated following *nipblb* knockdown or *NPMc*+ overexpression, indicating a hyper-activation of the canonical Wnt pathway (Figure 3A,B). To determine whether the Wnt signaling was enhanced specifically in hematopoietic cells, confocal images of the CHT of *Tg(TOPdGFP)* embryos were analyzed (Figure 3C). GFP+ cells were increased in both *nipblb*-MO- and *NPMc*+-injected embryos (10 increased/10 scored). Specifically, *nipblb* downregulation almost doubled the number of GFP+ cells in the CHT (n=27±5) in comparison to the number in controls (n=14±3), (Figure 3D,E, quantification in I). *NPMc*+ overexpression also increased the number of GFP+ cells in the CHT (n=20±4) in comparison to the number in controls (n=14±3), (Figure 3D-G, quantification in I). To further demonstrate that the increase of GFP+ cells in the CHT was due to the hyper-activation of the canonical Wnt pathway, we injected the

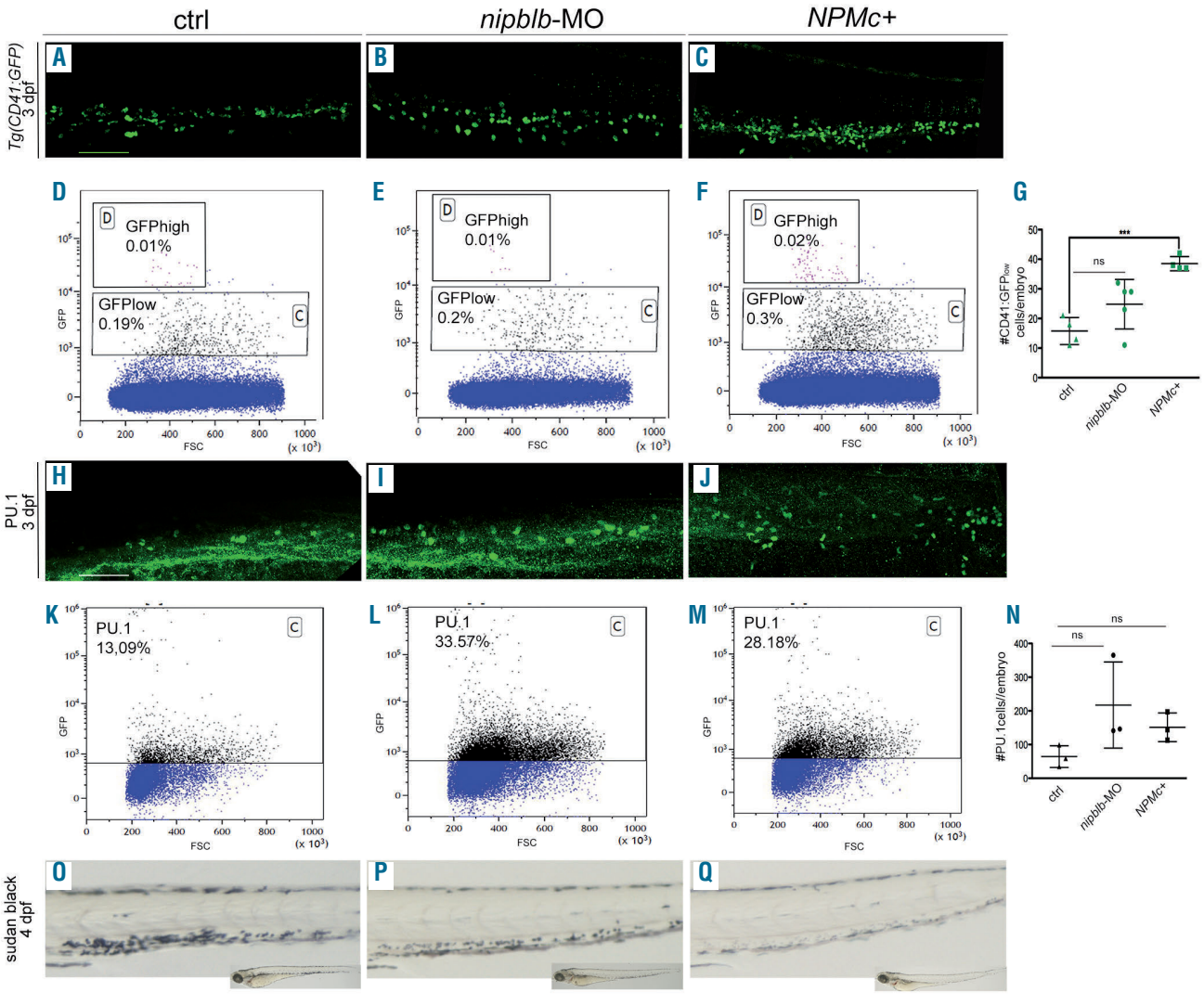

Figure 2. Myeloid cell differentiation is affected in *nipblb*-MO and *NPMc+* mRNA injected embryos. (A-C) Confocal analyses of *CD41:GFP* hematopoietic stem cells (HSC) from controls, *nipblb*-MO and *NPMc+* mRNA injected embryos at 3 days post-fertilization (dpf). The number of green fluorescent protein (GFP)-positive HSC was slightly increased in *nipblb*-MO, but significantly increased in *NPMc+* embryos in comparison to controls. (D-G) Fluorescence-activated cell sorting (FACS) analyses on GFP^{low}-positive HSC. (H-J) Confocal analyses of PU.1-positive myeloid precursor cells from controls, *nipblb*-MO and *NPMc+* mRNA injected embryos at 3 dpf. The numbers of GFP-positive myeloid precursors cells were increased in both *nipblb*-MO and *NPMc+* embryos in comparison to controls. (K-N) FACS analyses on Pu.1 GFP-positive cells. (O-Q) Sudan black staining for mature myeloid cells in controls, *nipblb*-MO and *NPMc+* mRNA injected embryos at 4 dpf. The mature myeloid cells were diminished in both *nipblb*-MO and *NPMc+* embryos in comparison to controls. Images were processed as described in the *Online Supplementary Methods*. The scale bar represents 100 μm. ***P<0.001. ns: non-significant; MO: morpholino; CHT: caudal hematopoietic tissue; ctrl: control.

Wnt inhibitor *dkk1b* mRNA (50 pg/embryo).[12] We validated the efficiency of *dkk1b* mRNA injection as the GFP$^+$ cells were diminished or absent in the hindbrain ventricle and in the CHT of the *Tg(TOPdGFP)* embryos in comparison to controls (*Online Supplementary Figure S5*). The co-injection of *dkk1b* in *nipblb*-MO or *NPMc+* mRNA-injected embryos rescued the number of GFP$^+$ cells in the CHT (10 rescued/10 scored for both) or even diminished the GFP$^+$ cells (n=8±3 for *nipblb*-MO/*dkk1b*; n=10±3 for *NPMc+/dkk1b*) (Figure 3F-H, quantification in I). Moreover, using the Wnt reporter line *Tg(TOPdGFP)* we verified that, following *nipblb*-MO injection, the canonical Wnt pathway appeared downregulated at 24 hpf but was then hyper-activated at 48 hpf (*Online Supplementary Figure S6*). This observation confirmed our previous work on a zebrafish model for *nipblb*-loss-of-function in which we observed downregulation of the canonical Wnt pathway at 24 hpf and correlated this with the neurological defect presented by patients affected by Cornelia de Lange syndrome (CdLS).[30]

Having seen hyper-activation of the canonical Wnt pathway in our zebrafish model with *nipblb* downregulation, we also analyzed this in humans with AML by measuring the expression of *AXIN2*, previously used as a reporter of canonical Wnt pathway activation in AML patients.[12] We did not observe a significant increase in *AXIN2* expression in our cohort of AML patients with *NIPBL* downregulation (*NIPBL* <1) in comparison to that in patients with normal or

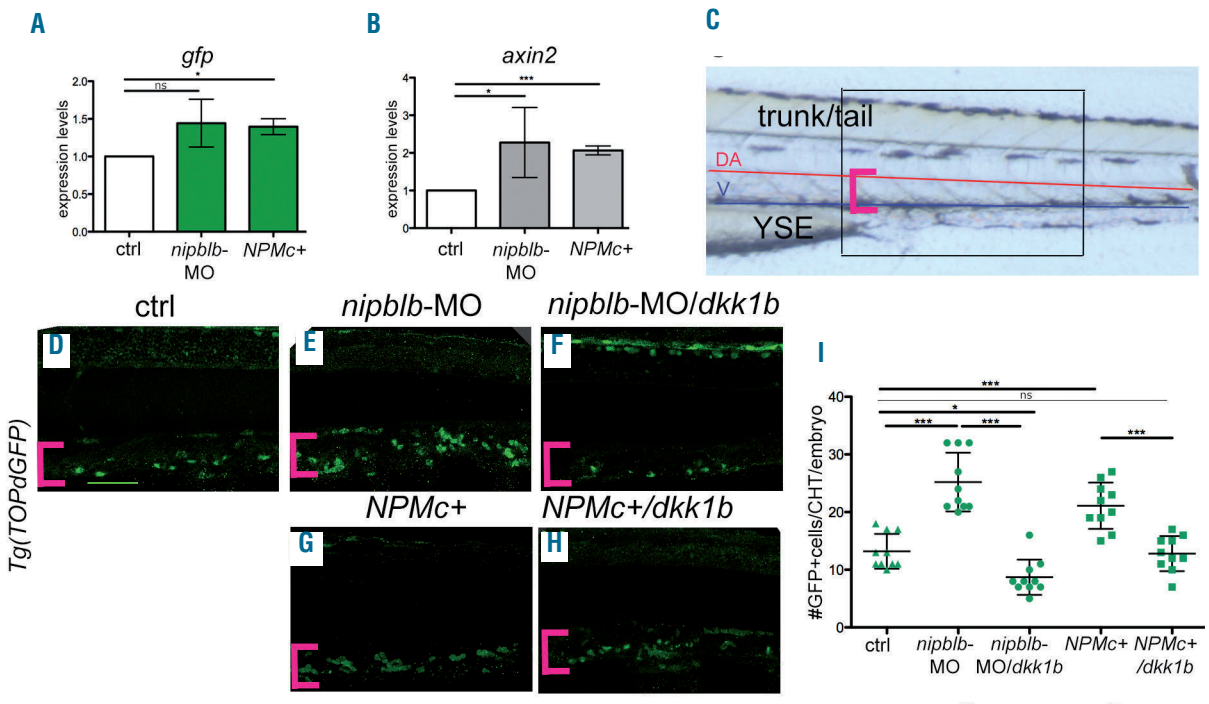

Figure 3. Canonical Wnt signaling is hyper activated in *nipblb*-MO and *NPMc+ Tg(TOPdGFP)* injected embryos at 3 days post-fertilization. (A, B) Quantitative reverse transcriptase polymerase chain reaction analyses of *gfp* and *axin2* expression in *nipblb*-MO and *NPMc+ Tg(TOPdGFP)* injected embryos indicated an increase of canonical Wnt activation status in comparison to that in controls. (C) Scheme of the trunk-tail region of embryos. Confocal images were always taken of the same region of the embryo, comprising the tip of the yolk sack extension (YSE) between the dorsal aorta (DA, red line) and the vein (V, blue line) as indicated by pink brackets. (D-H) Confocal images of the caudal hematopoietic tissue (CHT) of *Tg(TOPdGFP)* embryos injected with *nipblb*-MO (E) and NPMc+ mRNA (G) showed an increase of GFP+ cells in comparison to controls (D). Co-injection of the Wnt inhibitor *dkk1b* mRNA rescued the number of GFP+ cells (F-H). (I) Quantification of GFP+ cells in the selected region of the CHT. Images were processed as described in the *Online Supplementary Methods*. The scale bar represents 100 μm. **P*<0.05, ***P*<0.01 and ****P*<0.001. ns: non-significant; MO: morpholino; GFP: green fluorescent protein; ctrl: control.

increased expression of *NIPBL* (NIPBL>1) (*Online Supplementary Figure S7*). Further analyses in larger cohorts will be necessary to determine the correlation between *NIPBL* expression and the canonical Wnt pathway.

Hyper-activation of canonical Wnt signaling in hematopoietic stem cells impairs myeloid differentiation

To determine which type of hematopoietic cell in the CHT showed hyper-activation of the canonical Wnt pathway following *nipblb*-MO or *NPMc*+ mRNA injections, we sorted the CD41:GFP^{low} cells (0.8% control, 1% *nipblb*-MO, 1.1% *NPMc*+) from 3 dpf embryos injected with *nipblb*-MO or *NPMc*+ mRNA and observed a modest increase in *axin2* expression in these cells in comparison to the expression in CD41:GFP^{low} cells from controls (Figure 4A-A'''). Moreover, we performed immunofluorescence staining with the Active β-catenin (Active β-cat) antibody for the Wnt pathway and GFP antibody for HSC cells of the CD41:GFP embryos. The number of GFP/Active β-cat double-positive cells present in the CHT of 3-dpf embryos injected with *nipblb*-MO or *NPMc*+ mRNA (5 double-positive cells indicated by the arrows in the CHT of Figure 4C"-D") was higher than that in controls (2 double-positive cells indicated by the arrows in the CHT of Figure 4B"), demonstrating that the Wnt pathway was activated specifically in HSC (Figure 4B-D").

The myeloid differentiation defects presented by *nipblb*-MO and *NPMc*+ mRNA injected embryos at 3 dpf were caused by hyper-activation of the canonical Wnt pathway. Inhibiting this pathway, either by *dkk1b* mRNA injection or by treatment with the Wnt pharmacological inhibitor indomethacin,[26] rescued the hematopoietic phenotype. Indeed, by WISH we showed that the increased number of myeloid precursors positive for *spi1b* observed in *nipblb*-MO or *NPMc*+ mRNA injected embryos, returned to levels comparable to those in controls (Figure 5A-G).

NPMc+ and *nipblb* cooperation in the hyper-activation of canonical Wnt signaling and myeloid defects

The evidence that we had collected so far showed that *NPMc*+ downregulates *NIPBL*, both in human AML patients and in zebrafish. We also demonstrated that dysregulation of both genes impairs myeloid differentiation through hyper-activation of the canonical Wnt pathway. To further address a possible cooperation between the two genes, we performed dose-response assays. We injected subcritical doses of *nipblb*-MO (0.6 pmol/embryo) or *NPMc*+ mRNA (50 pg/embryo), which singularly did not cause an increase in GFP+ cells in the CHT of *Tg(TOPdGFP)* embryos (Figure 6B,C) in comparison to controls (Figure 6A, quantification in E), or in *spi1b*-positive myeloid progenitors (Figure 6G,H) in comparison to the number of cells in controls (Figure 6F, quantification in J). When co-injected, subcritical doses of *nipblb*-MO/NPMc+ mRNA recapitulated the phenotype previously observed following injections of full doses, with an

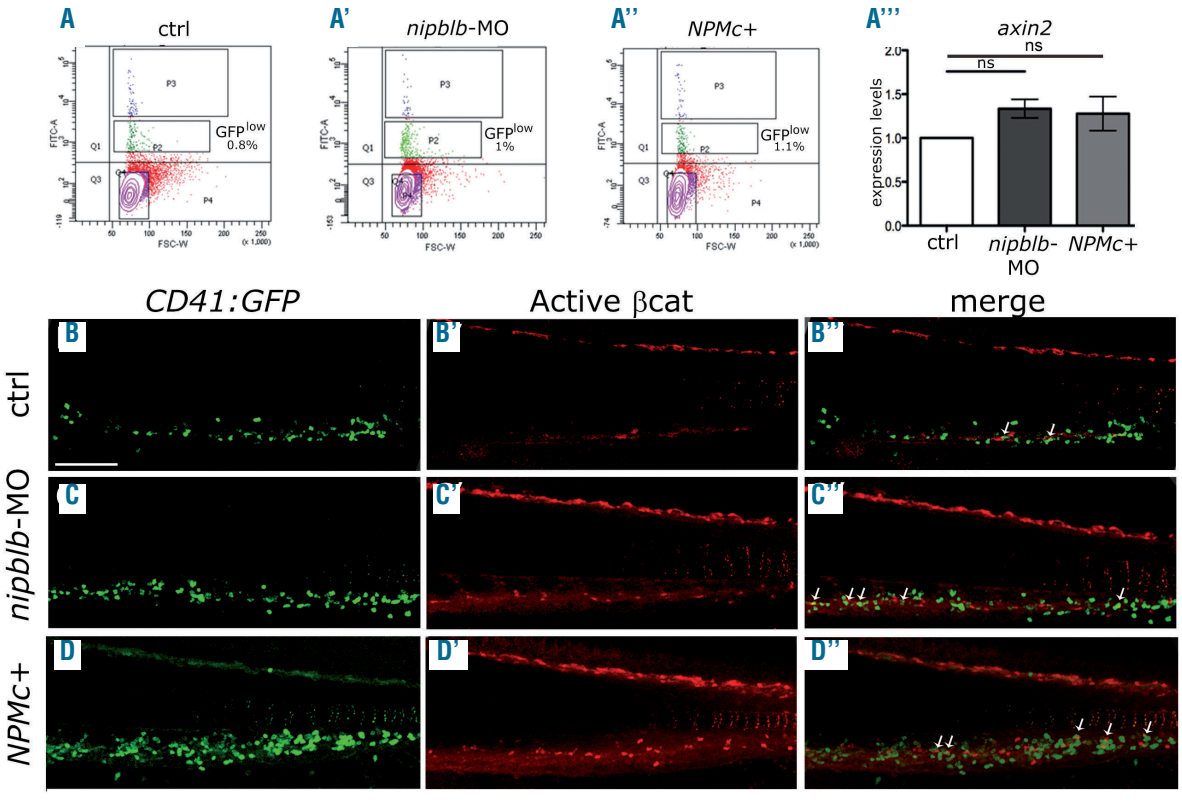

Figure 4. The canonical Wnt pathway is hyper-activated specifically in hematopoietic stem cells. (A-A'') Fluorescence-activated cell sorting analysis of CD41:GFP^{low} cells from controls (A), *nipblb*-MO (A') and *NPMc+* mRNA (A'') injected embryos at 3 days post-fertilization (dpf) and quantitative reverse transcriptase polymerase chain reaction analysis of *axin2* expression on sorted cells (A'''). (B-D'') Immunofluorescence staining with green fluorescent protein (GFP) for hematopoietic stem cells. (B-D) and Active β-catenin for Wnt activation (Active β-cat) (B'-D') antibodies. Merging of the two signals (B''-D'') showed an increased number of GFP/Active β-cat double-positive cells (arrows) at 3 dpf in the caudal hematopoietic tissue of embryos injected with *nipblb*-MO or *NPMc+* mRNA in comparison to the number in controls. Images were processed as described in the *Online Supplementary Methods*. The scale bar represents 100 μm. *P<0.05. ns: non-significant; ctrl: control; MO: morpholino.

increased number of GFP$^+$ cells in the CHT of the *Tg(TOPdGFP)* embryos and an enhanced expression of *spi1b* (Figure 6F-I, quantification of the phenotypes in J), indicating a cooperation between *NPMc+* and *nipblb* downregulation.

Discussion

In this work, we built on the observation that, in addition to the cohesin mutations detected in 10% of patients with myeloid malignancies, low expression of cohesin genes was present in an additional 15% of patients showing similar expression signatures as those with somatic cohesin mutations.[28] We therefore investigated the expression of cohesin genes in our cohort of 40 adult AML patients divided according to the absence/presence of *NPM1* mutation. We chose to analyze *NPM1* mutations as they are pivotal in AML but likely insufficient by themselves to cause malignant transformation, requiring the co-occurrence of other mutations such as *FLT3*-ITD or *RAS*.[9,34] In addition, a correlation between *NPM1* mutations and somatic mutations in cohesin genes has already been reported,[28] although the specific loss-of-function of cohesins has never been investigated in association with *NPM1* mutations. Among the cohesin genes analyzed in our cohort of adult AML patients, we found that only *NIPBL* showed a lower expression when *NPM1* was mutated. NIPBL is a regulator of the cohesin complex deputed to loading the complex onto double-stranded DNA. However, previous studies suggested a specific activity of NIPBL in gene transcription regulation and NIPBL binding sites, which do not overlap with those of cohesins, were identified *in vitro*.[35] We, therefore, decided to analyze the effects of *NIPBL* downregulation on myeloid differentiation. The zebrafish represents an ideal model for studying the function of cohesin genes as knockdown can be achieved by the injection of specific oligonucleotide antisense morpholino.[30] Investigating the effects of *nipblb*-loss-of-function during zebrafish definitive hematopoiesis, we observed an increased number of myeloid progenitors. Similar results have been obtained in different models of cohesin loss-of-function. For example, in murine models the use of short hairpin RNA against *Stag2* and *Smc3* generated a maturation block, delayed differentiation, and enhanced renewal of HSC, similar to the events occurring in myeloid neoplasms.[36] In another study, RNA interference mouse models were created with inducible knockdown of *Rad21*, *Smc1a* and *Stag2*, leading to a shift in the hematopoietic stem compartment, an increased replating capacity and, over time, the development of clinical features of myeloproliferative neoplasms.[18] Unlike *STAG2*, *SMC3*, *SMC1A*, and *RAD21*, *NIPBL* is not a recurrently mutated gene in AML.[28] In

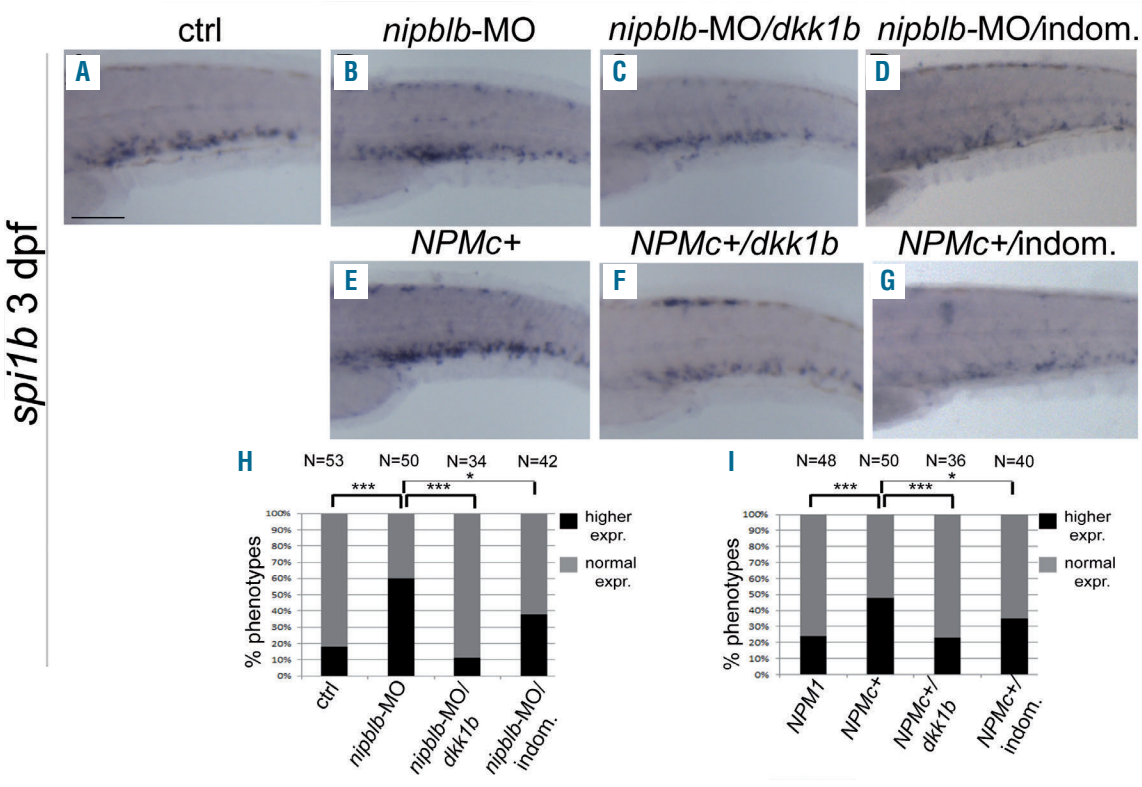

Figure 5. The impairment of myeloid cell differentiation in *nipblb*-MO and *NPMc+* injected embryos is caused by hyper-activation of canonical Wnt signaling. (A-G) Whole mount *in situ* hybridization analyses of *spi1b*. The expression of *spi1b* was increased in *nipblb*-MO (B) and *NPMc+*-injected embryos (E) in comparison to that in controls (A). The myeloid phenotype was rescued by injection of Wnt inhibitor *dkk1b* mRNA (C, F) and treatment with indomethacin (D, G). Quantification of the observed phenotypes in (H) and (I). Images were processed as described in the *Online Supplementary Methods*. The scale bar represents 100 μm. **P*<0.05 and ****P*<0.001. ctrl: control; MO: morpholino.

humans, heterozygous loss-of-function mutations of *NIPBL* cause CdLS.[37] Nevertheless, CdLS patients with mutations in *NIPBL* or in other cohesin genes are not predisposed to myeloid neoplasms. Rare cases of leukemia have been reported in patients with CdLS, but were probably caused by other inherent aspects of this latter pathology.[38–40] The mutations in cohesin genes responsible for CdLS and leukemia insurgence are considered different for their pathophysiological output: cohesin mutations in tumors occur in somatic adult cells while germline cohesin mutations in CdLS patients occur in embryonic tissue. Moreover, cohesin mutations in cancer might not trigger, but contribute to tumorigenesis only with other mutations such as *TET2*,[41] *NPM1*,[9,42] *DNMT3A*[43] or *FLT3*-ITD.[44] Indeed, we speculate that the decrease in *NIPBL* expression observed in AML patients might not be due to specific somatic mutations occurring at the gene level, but rather to a secondary effect caused by genetic lesions that have arisen elsewhere (i.e., *NPM1*).

In *nipblb*-loss-of-function embryos we observed defects in myeloid differentiation with an increased number of myeloid progenitors and a decrease of mature myeloid cells. These hematopoietic defects share similarities with the myeloproliferative phenotype of *NPMc+* embryos.[12,13] Indeed, we also confirmed that the forced expression of *NPMc+* generated a phenotype with expansion of HSC and myeloid precursors. However, the main difference in the hematopoietic phenotype generated by *nipblb* knockdown and *NPMc+* forced expression was in the HSC population. In this regard, while HSC numbers were significantly increased in *NPMc+* embryos, in *nipblb*-MO injected embryos they were almost comparable to those in controls. This finding is not surprising as we demonstrated that *nipblb* acts downstream of, and is regulated by, *NPMc+*. It is therefore conceivable that, also in the hematopoietic cascade that drives myeloid differentiation, the effects of *nipblb* are exerted on a population derived from HSC, such as myeloid progenitors.

We further observed that in *nipblb* knockdown and *NPMc+* overexpressed zebrafish embryos, the Wnt/β-catenin pathway was hyper-activated. In the process of hematopoiesis, many signaling pathways are critical during the different developmental stages of HSC and for the maturation of these cells into differentiated lineages. In particular, the canonical Wnt pathway exerts its action on specific cell populations, being fine-tuned in a dosage-dependent fashion.[45] We demonstrated that Nipbl plays an active role in this modulation. Indeed, in a previous study, we showed that the downregulation of *nipblb* in zebrafish embryos at 24 hpf led to decreased activation of the canonical Wnt pathway.[30] In this work we demonstrated that, from 48 hpf, Nipbl acts in an opposite way by hyper-activating the Wnt pathway in the whole embryo. It is conceivable that, given its double effects on the Wnt pathway, Nipblb might be considered a new factor in canonical Wnt pathway modulation.

Recently several Wnt inhibitors have been identified as potential drugs to reduce tumor cell viability in lymphoma and myeloma cell lines *in vitro* and *in vivo*.[46] Thus, Wnt/β-catenin inhibitors, such as indomethacin that has already

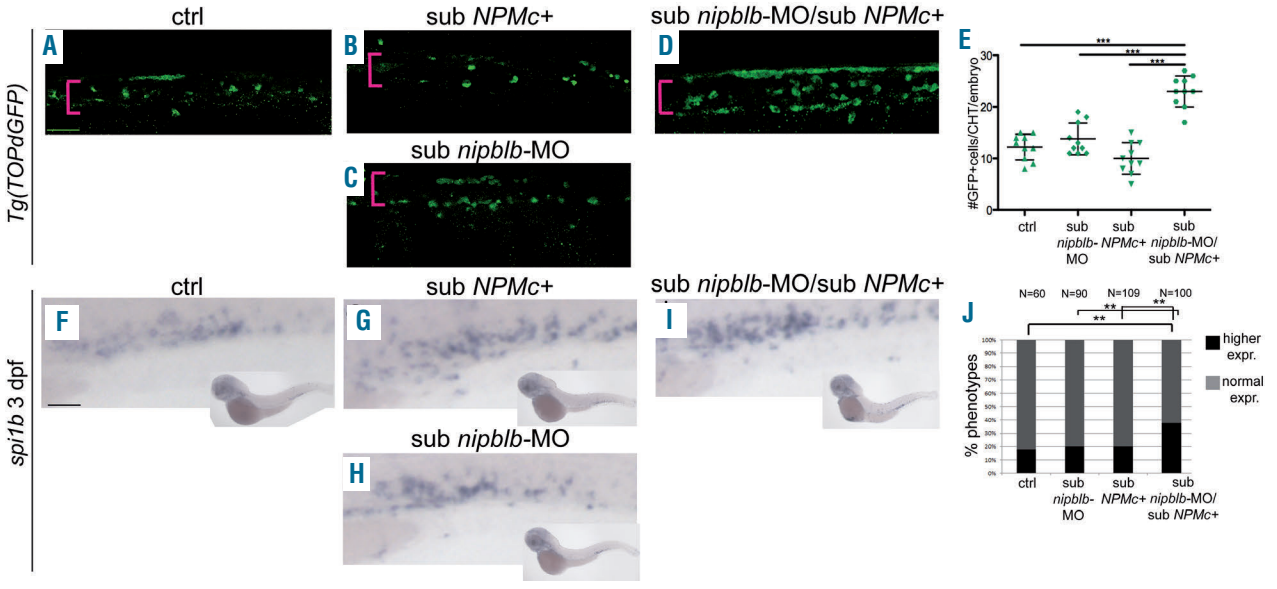

Figure 6. Co-injection of subcritical doses of *nipblb*-MO and *NPMc+*, which singularly do not have effects, indicates cooperation between *NPMc+* and *nipblb* in myeloid differentiation. (A-D) The number of green fluorescent protein (GFP)$^+$ cells in caudal hematopoietic tissue (CHT) was increased when embryos at 3 dpf were co-injected with subcritical doses of both *nipblb*-MO and *NPMc+* mRNA (D) in comparison to a single injection of a subcritical dose of *NPMc+* mRNA (B) or *nipblb*-MO (C). The numbers of GFP$^+$ cells in the CHT following the single injections were comparable to those in the controls (A). (E) Quantification of GFP$^+$ cells in the CHT. (F-I) Whole mount in situ hybridization analyses of the myeloid precursor marker *spi1b*. *spi1b* expression was increased in embryos co-injected with subcritical doses of both *nipblb*-MO and *NPMc+* mRNA (I) in comparison to the expression in controls and embryos injected with a subcritical dose of either *NPMc+* (sub *NPMc+*) (G) or *nipblb*-MO (sub *nipblb*-MO) (H). (J) Quantification of the embryos presenting increased *spi1b* expression. Images were processed as described in the *Online Supplementary Methods*. The scale bar represents 100 μm. $^{**}P<0.01$ and $^{***}P<0.001$. ctrl: control; MO: morpholino.

been investigated in clinical trials[26] and was able to rescue the hematopoietic phenotype in our study, could be attractive candidates for the development of new treatments for *NPMc+* AML patients.

Further analyses are necessary to investigate the mechanisms through which NPMc+ interacts with *NIPBL* and how they regulate the canonical Wnt pathway and the hematopoietic phenotype. One hypothesis raised by previous research and our analyses is the involvement of other members of the cohesin complex such as Rad21, which is negatively regulated by Nipbl in both murine fibroblasts[47] and zebrafish (see Figure 1F). Alternatively, the aberrant cytoplasmic dislocation of mutant *NPM1* might alter the normal regulation of *NIPBL* expression in the nucleus, similarly to what happens in the important *PU.1-NPM1*-mediated regulation in myeloid precursors.[48] Large scale transcriptomic and/or proteomic analyses will be useful to unravel the mechanism and, to this purpose, the use of the zebrafish platform with cohesin knockdown might be a suitable model system.

In conclusion, our study correlates *NIPBL* with *NPM1* mutations in adult AML patients for the first time and demonstrates their interplay in myeloid cell differentiation in zebrafish through involvement of the canonical Wnt pathway. The results obtained will foster the identification of new potential targets for the treatment of subgroups of AML.

Acknowledgments

We thank R Monteiro, (University of Birmingham), for the Tg(CD41:GFP/kdrl:dsRED) zebrafish line, N. Bolli, (University of Milan) for useful discussion of the data, the cytometry desk staff (IFOM, Milan) for technical help in FACS experiments, MC Crosti of the INGM FACS facility for sorting experiments and M Spreafico and M Cafora (University of Milan) for their priceless support in experimental procedures. This work was supported by the Associazione Italiana per la Ricerca sul Cancro (AIRC) (MFAG#18714). The funders had no role in the study design, data collection and interpretation, or the decision to submit the work for publication.

References

1. Löwenberg B, Downing JR, Burnett A. Acute myeloid leukemia. N Engl J Med. 1999;341(14):1051–1062.
2. Ley TJ, Mardis ER, Ding L, et al. DNA sequencing of a cytogenetically normal acute myeloid leukaemia genome. Nature. 2008;456(7218):66–72.
3. Yan X-J, Xu J, Gu Z-H, et al. Exome sequencing identifies somatic mutations of DNA methyltransferase gene DNMT3A in acute monocytic leukemia. Nat Genet. 2011;43(4):309–315.
4. Corces-Zimmerman MR, Majeti R. Preleukemic evolution of hematopoietic stem cells: the importance of early mutations in leukemogenesis. Leukemia. 2014;28(12):2276–2282.
5. Cancer Genome Atlas Research Network, Ley TJ, Miller C, Ding L, et al. Genomic and epigenomic landscapes of adult de novo acute myeloid leukemia. N Engl J Med. 2013;368(22):2059–2074.
6. Borer RA, Lehner CF, Eppenberger HM, Nigg EA. Major nucleolar proteins shuttle between nucleus and cytoplasm. Cell. 1989;56(3):379–390.
7. Dumbar TS, Gentry GA, Olson MOJ. Interaction of nucleolar phosphoprotein B23 with nucleic acids. Biochemistry. 1989;28(24):9495–9501.
8. Cheng K, Grisendi S, Clohessy JG, et al. The leukemia-associated cytoplasmic nucleophosmin mutant is an oncogene with paradoxical functions: Arf inactivation and induction of cellular senescence. Oncogene.

2007;26(53):7391–7400.
9. Vassiliou GS, Cooper JL, Rad R, et al. Mutant nucleophosmin and cooperating pathways drive leukemia initiation and progression in mice. Nat Genet. 2011;43(5):470–476.
10. Alcalay M, Tiacci E, Bergomas R, et al. Acute myeloid leukemia bearing cytoplasmic nucleophosmin (NPMc+AML) shows a distinct gene expression profile characterized by up-regulation of genes involved in stem-cell maintenance. Blood. 2005;106(3):899–902.
11. Mallardo M, Caronno A, Pruneri G, et al. NPMc+ and FLT3-ITD mutations cooperate in inducing acute leukaemia in a novel mouse model. Leukemia. 2013;27(11):2248–2251.
12. Barbieri E, Deflorian G, Pezzimenti F, et al. Nucleophosmin leukemogenic mutant activates Wnt signaling during zebrafish development. Oncotarget. 2016;7(34):55302–55312.
13. Bolli N, Payne EM, Grabher C, et al. Expression of the cytoplasmic NPM1 mutant (NPMc+) causes the expansion of hematopoietic cells in zebrafish. Blood. 2010;115(16):3329–3340.
14. Zhang J, Niu C, Ye L, et al. Identification of the haematopoietic stem cell niche and control of the niche size. Nature. 2003;425(6960):836–841.
15. Thota S, Viny AD, Makishima H, et al. Genetic alterations of the cohesin complex genes in myeloid malignancies. Blood. 2014;124(11):1790–1798.
16. Kagey MH, Newman JJ, Bilodeau S, et al. Mediator and cohesin connect gene expression and chromatin architecture. Nature. 2010;467(7314):430–435.
17. Solomon DA, Kim T, Diaz-Martinez LA, et al. Mutational inactivation of STAG2 causes aneuploidy in human cancer. Science. 2011;333(6045):1039–1043.
18. Mullenders J, Aranda-Orgilles B, Lhoumaud P, et al. Cohesin loss alters adult hematopoietic stem cell homeostasis, leading to myeloproliferative neoplasms. J Exp Med. 2015;212(11):1833–1850.
19. de Leval L, Waltregny D, Boniver J, Young RH, Castronovo V, Oliva E. Use of histone deacetylase 8 (HDAC8), a new marker of smooth muscle differentiation, in the classification of mesenchymal tumors of the uterus. Am J Surg Pathol. 2006;30(3):319–327.
20. Mazumdar C, Majeti R. The role of mutations in the cohesin complex in acute myeloid leukemia. Int J Hematol. 2017;105(1):31–36.
21. Fisher JB, Peterson J, Reimer M, et al. The cohesin subunit Rad21 is a negative regulator of hematopoietic self-renewal through epigenetic repression of Hoxa7 and Hoxa9. Leukemia. 2017;31(3):712–719.
22. Thisse C, Thisse B. High-resolution in situ hybridization to whole-mount zebrafish embryos. Nat Protoc. 2008;3(1):59–69.
23. Brusegan C, Pistocchi A, Frassine A, della Noce I, Schepis F, Cotelli F. Ccdc80-l1 is involved in axon pathfinding of zebrafish motoneurons. PLoS One. 2012;7(2):e31851.
24. Cvejic A, Serbanovic-Canic J, Stemple DL, Ouwehand WH. The role of meis1 in primitive and definitive hematopoiesis during zebrafish development. Haematologica. 2011;96(2):190–198.
25. Bresciani E, Broadbridge E LP. An efficient dissociation protocol for generation of single cell suspension from zebrafish embryos and larvae. MethodsX 2018;5:1287–1290.
26. North TE, Goessling W, Walkley CR, et al. Prostaglandin E2 regulates vertebrate haematopoietic stem cell homeostasis. Nature. 2007;447(7147):1007–1011.
27. Livak KJ, Schmittgen TD. Analysis of relative gene expression data using real-time quantitative PCR and the 2(-delta delta C(T)) method. Methods. 2001;25(4):402–408.
28. Thol F, Bollin R, Gehlhaar M, et al. Mutations in the cohesin complex in acute myeloid leukemia: clinical and prognostic implications. Blood. 2014;123(6):914–920.
29. Muto A, Calof AL, Lander AD, Schilling TF. Multifactorial origins of heart and gut defects in Nipbl-deficient zebrafish, a model of Cornelia de Lange syndrome. PLoS Biol. 2011;9(10):e1001181.
30. Pistocchi A, Fazio G, Cereda A, et al. Cornelia de Lange syndrome: NIPBL haploinsufficiency downregulates canonical Wnt pathway in zebrafish embryos and patients fibroblasts. Cell Death Dis. 2013;4(10):e866.
31. Lin HF, Traver D, Zhu H, et al. Analysis of thrombocyte development in CD41-GFP transgenic zebrafish. Blood. 2005;106(12):3803–3810.
32. Dorsky RI, Sheldahl LC, Moon RT. A Transgenic lef1/β-catenin-dependent reporter is expressed in spatially restricted domains throughout zebrafish development. Dev Biol. 2002;241(2):229–237.
33. Jho E, Zhang T, Domon C, Joo C-K, Freund J-N, Costantini F. Wnt/beta-catenin/Tcf signaling induces the transcription of Axin2, a negative regulator of the signaling pathway. Mol Cell Biol. 2002;22(4):1172–1183.
34. Dovey OM, Cooper JL, Mupo A, et al. Molecular synergy underlies the co-occurrence patterns and phenotype of NPM1-mutant acute myeloid leukemia. Blood. 2017;130(17):1911–1922.
35. Zuin J, Franke V, van IJcken WFJ, et al. A cohesin-independent role for NIPBL at promoters provides insights in CdLS. PLoS Genet. 2014;10(2):e1004153.
36. Galeev R, Baudet A, Kumar P, et al. Genome-wide RNAi screen identifies cohesin genes as modifiers of renewal and differentiation in human HSCs. Cell Rep. 2016;14(12):2988–3000.
37. Tonkin ET, Wang TJ, Lisgo S, Bamshad MJ, Strachan T. NIPBL, encoding a homolog of fungal Scc2-type sister chromatid cohesion proteins and fly Nipped-B, is mutated in Cornelia de Lange syndrome. Nat Genet. 2004;36(6):636–641.
38. Schrier SA, Sherer I, Deardorff MA, et al. Causes of death and autopsy findings in a large study cohort of individuals with Cornelia de Lange syndrome and review of the literature. Am J Med Genet A. 2011;155(12):3007–3024.
39. Deardorff MA, Bando M, Nakato R, et al. HDAC8 mutations in Cornelia de Lange syndrome affect the cohesin acetylation cycle. Nature. 2012;489(7415):313–317.
40. Vial Y, Lachenaud J, Verloes A, et al. Down syndrome-like acute megakaryoblastic leukemia in a patient with Cornelia de Lange syndrome. Haematologica. 2018;103(6):274.
41. Moran-Crusio K, Reavie L, Shih A, et al. Tet2 loss leads to increased hematopoietic stem cell self-renewal and myeloid transformation. Cancer Cell. 2011;20(1):11–24.
42. Grisendi S, Bernardi R, Rossi M, et al. Role of nucleophosmin in embryonic development and tumorigenesis. Nature. 2005;437(7055):147–153.
43. Challen GA. Dominating the negative: how DNMT3A mutations contribute to AML pathogenesis. Cell Stem Cell. 2017;20(1):7–8.
44. Viny AD, Ott CJ, Spitzer B, et al. Dose-dependent role of the cohesin complex in normal and malignant hematopoiesis. J Exp Med. 2015;212(11):1819–1832.
45. Trompouki E, Bowman T V., Lawton LN, et al. Lineage regulators direct BMP and Wnt pathways to cell-specific programs during differentiation and regeneration. Cell. 2011;147(3):577–589.
46. Ma S, Yang LL, Niu T, et al. SKLB-677, an FLT3 and Wnt/β-catenin signaling inhibitor, displays potent activity in models of FLT3-driven AML. Sci Rep. 2015;515646.
47. Newkirk DA, Chen YY, Chien R, et al. The effect of Nipped-B-like (Nipbl) haploinsufficiency on genome-wide cohesin binding and target gene expression: modeling Cornelia de Lange syndrome. Clin Epigenetics. 2017;9:89.
48. Gu X, Ebrahem Q, Mahfouz RZ, et al. Leukemogenic nucleophosmin mutation disrupts the transcription factor hub that regulates granulomonocytic fates. J Clin Invest. 2018;128(10):4260–4279.